HHS Public Access

Author manuscript

J Vasc Surg. Author manuscript; available in PMC 2018 July 01.

Published in final edited form as:

J Vasc Surg. 2017 July ; 66(1): 232–242.e4. doi:10.1016/j.jvs.2016.07.105.

A novel chronic advanced staged abdominal aortic aneurysm murine model

Guanyi Lu, MD, PhD[a], **Gang Su, MD**[a], **John P Davis, MD**[a], **Basil Schaheen, MD**[a], **Emily Downs, MD**[a], **R Jack Roy, BS**[b], **Gorav Ailawadi, MD**[a], and **Gilbert R Upchurch Jr, MD**[a]

[a]Department of Surgery, University of Virginia, Charlottesville, VA

[b]Molecular Imaging Core, Department of Radiology, University of Virginia, Charlottesville, VA

Abstract

Objective—The purpose of this study was to establish a reliable, chronic model of abdominal aortic aneurysm (AAA).

Materials and methods—120 eight-week old C56BL/6 male mice were equally divided into three groups: 1) BAPN Group: 0.2% 3-aminopropionitrile fumarate salt (BAPN) drinking water was provided to mice two days before surgery until the end of study. Sham aneurysm induction surgery was performed using 5 μl of heat de-activated elastase. 2) Elastase Group: Mice were given regular drinking water without BAPN. During aneurysm induction surgery, 5 μl of active form elastase (10.3mg protein/ml, 5.9units/mg protein) was applied on top of adventitia of infrarenal abdominal aorta for 5 minutes. 3) BAPN+Elastase Group: Mice were given both BAPN drinking water and active form of elastase application as above. On post-operative days 7, 14, 21, 28 and 100, aortic samples were collected for histology, cytokine array and gelatin zymography after aortic diameter measurement.

Results—Compared with Elastase group, BAPN+Elastase group had higher AAA formation rate (93% vs 65%, $P < .01$) with more advanced-staged AAAs (25/42 vs 1/40 for Stage II & III, $P < .001$). Aneurysms from the BAPN+Elastase Group demonstrated persistent long-term growth (221.5 ± 36.6%, 285.8 ± 78.6%, 801 ± 160% on day 21, 28 and 100 respectively, $P < .001$), with considerable thrombus formation (54%) and rupture (31%) at the advanced stages of AAA development. Cytokine levels (pro-MMP9, IL-1β, IL-6, CCL-5, TREM-1, MCP-1 and TIMP-1) in BAPN+Elastase Group were higher than Elastase Group on day 7. After day 7, cytokine levels returned to baseline with the exception of elevated MMP2 activity. By histology, $CD3^+$T cells in the BAPN+Elastase Group were elevated on days 28 and 100.

Conclusions—A combination of oral BAPN administration and peri-aortic elastase application induced a chronic, advanced staged AAA with characteristics of persistent aneurysm growth,

Correspondence: Gilbert R Upchurch Jr, MD, Department of Surgery, University of Virginia Health System, PO Box 800679, Charlottesville, VA 22908. gru6n@virginia.edu. Tel: 434-243-6334. Fax: 434-243-9941.

Author conflict of interest: None.

thrombus formation, and spontaneous rupture. Future studies should utilize this model, especially for examining tissue remodeling during the late stages of aneurysm development.

INTRODUCTION

Aortic aneurysms are a chronic, end-stage disease of the aortic wall. Investigation of human aneurysm formation is relatively difficult due to the following: 1) aneurysm formation usually is asymptomatic; 2) inflammation isolated in the aortic wall has little or no circulatory biomarkers to date; and 3) limited samples from open surgery or autopsy represent only end-staged AAA. Although there are many animal models available for AAA study[1–6], none of these models closely represents all the pathological characteristics of human AAA. For example, most of these AAA models are acute or sub-acute. If followed long enough, AAAs in these models tend to regress soon after formation, similar to an acute wound healing process. The goal of the present study was to establish a reliable, chronic AAA animal model that provides stable, advanced staged infrarenal AAA.

MATERIAL AND METHODS

1. Experimental design

Experiment #1: Development of chronic AAA model—120 eight-week old wild type C56BL/6 male mice (Jackson Lab, Bar Harbor, Maine) were equally divided into three groups. 1) BAPN Group: 3-aminopropionitrile fumarate salt (Sigma Aldrich, St. Louis, MO) was dissolved in drinking water at 0.2% concentration and provided to the mice two days before surgery until the end of the study. Sham aneurysm induction surgery was performed by using 5 μl of heat de-activated (100°C for 30 minutes) elastase to replace active form of elastase. The rest of the surgical procedure was the same as the other two groups. 2) Elastase Group: Mice were provided with regular drinking water. General anesthesia was achieved with isoflurance inhalation. The lower ¾ of the infrarenal abdominal aorta was exposed circumferencely and separated from vena cava. The upper ¼ of the infrarenal abdominal aorta (about 2mm below the left renal artery) and surrounding tissue was left intact. The vena cava and separated tissues were push to each side, leaving the exposed aorta at the bottom of the boat-shape area. Using pipette with a fine tip, 5 μl of elastase (Sigma Aldrich, St. Louis, MO, 10.3mg protein/ml, 5.9units/mg protein) was applied topically to the exposed aortic adventitia. The whole section of the exposed aorta was soaked into the elastase for 5 minutes. Do not overfill the exposed area, so the elastase digestion on the aorta was confined within the exposed area. The intact area had no direct contact with elastase. After 5 minutes, the exposed area was washed gently with normal saline solution and dried with cotton-tip applicators. All the surgical procedures were performed by one surgeon to minimize the technical variables. Abdomen was closed routinely and mouse was recovered. 3) BAPN +Elastase Group: Mice were given both BAPN in the drinking water as BAPN Group, as well as aneurysm induction surgery as Elastase Group.

At post-operative days 7, 14, 21, 28 and 100, eight mice from each group were euthanized under anesthesia by overdose and exsanguination. The abdominal aorta was dissected to expose the induced AAA. A short section of intact aorta just above the induced AAA was used as a self-control. Aortic diameter was measured using video microscopy with NIS-

Elements D.3.10 software attached to the microscope (Nikon SMX-800, Melville, NY). Aortic dilation was determined using (maximal AAA diameter – self-control aortic diameter)/maximal AAA diameter × 100%. A dilation of 100% or more was considered to be positive for AAA.

Aortic samples also were graded using the following stages of aneurysm formation. *Negative* (−): Symmetric dilation <100%, thin wall, no thrombus/rupture. *Stage I* (+): Symmetric dilation between 100–200%, thick wall, no thrombus/rupture. *Stage II* (++): Asymmetric dilation >200%, thick/uneven wall, no thrombus/rupture. *Stage III* (+++): *Stage II* plus thrombus/rupture (Fig 1). After aortic diameter measurement and grading, abdominal aorta samples were collected for cytokine screening (array, n=8/time point/group) and quantification analysis (gelatin zymography, Western blot or ELISA, n=5/time point/group) and histology (n=3/time point/group).

In order to observe long-term growing trends of the aneurysm, the end point of our experiments was extended to 100 days post-surgery. Due to the significant number of aneurysm ruptures, 6 extra mice were added in BAPN+Elastase Group. Aortic samples were measured and collected at the end of experiment or at the time of AAA rupture, whichever happened earlier. An additional group of 8 naive C56BL/6 male mice were sacrificed and the aorta samples were used as pre-surgery baseline controls for the above three groups.

Experiment #2: Impact of age on AAA formation—In order to determine the effects of animal's age on AAA formation, three groups of geriatric mice of different age were used to compare with young mice (8-week old). Each group consisted of 6 or more C56BL/6 male mice. The aged groups included mice that were 6, 12 and 18 months old, respectively. AAA was induced the same way as the Elastase Group in the Experiment #1 described above. Aortic and blood samples were harvested on day 14 post-surgery after aortic diameter measurement.

To exclude the dietary variable, mice in all experiments were feed with minimal phytoestrogen diet (2016 Teklad Grobal 16% Protein Rodent Diet, Harlan Labs Inc, Frederick, MD). All the above experiments were conducted in accordance with standards approved by the Animal Care and Use Committee of University of Virginia (#3848).

2. Histology and immunohistochemical staining

Aortic specimens were fixed in 4% buffered formaldehyde for 24 hours, transferred to 70% ethanol, and subsequently embedded in paraffin. Aortic cross-sections were stained with Verhoeff-Van Gieson or picrosirius red staining for elastin and collagen, respectively. Immunohistochemical stainings for neutrophils, migratory macrophages, $CD3^+$ T cells and smooth muscle actin (α-SMA) were performed as published[7–9]. For grading, integrated optical density value of positive staining area of each section was randomly selected and measured. Four randomly selected 20× fields per section were assessed for the density of staining by a blinded observer. Total number of $CD3^+$ T cells per cross-section was also counted for each sample.

3. Angiogenesis and cytokines arrays

Protein from aortic samples was isolated as described earlier [10]. Pooled protein samples (30 μg, from 8 mice/time point/group) were used in proteome profiler cytokine array and proteome profiler angiogenesis array according to manufacturer's instruction (R & D Systems, cat# ARY 006, ARY 015, Minneapolis, MN). All samples were run in duplicate and mean value was used to represent each cytokine level.

4. Zymography

Using protein isolated from the aortic samples, gelatin zymography was performed to determine MMP2 and MMP9 activity. Precast zymography gels (10%, Invitrogen, Carlsbad, CA) were loaded with 3μg of tissue protein from each aortic sample diluted into 2× Tris-glycine SDS sample buffer and electrophoretically separated under non-reducing conditions. The gels were renatured for 30 minutes in renaturing buffer (Invitrogen) and incubated in developing buffer (Invitrogen, Carlsbad, CA) for 24 hours at 37 ° C rocker. The gels were then stained in Simply Blue Safe Stain (Invitrogen, Carlsbad, CA). Pro and active forms of MMP2 and MMP9 appeared as clear band against the blue background. Quantification was determined according the optical density using Bio-Rad Image Lab Software version 4.0.

5. ELISA and Western blot

ELISA analyses were done for IL-1β, IL-6, MCP-1, RANTES and TREM-1 quantification according to manufacturer's instructions (BD Biosciencecs Pharmingen, San Diego, CA). Protein samples (10ug/well) extracted from mouse aortic tissue were used for each cytokine. Western blot was used for TIMP-1 analysis (primary antibody 1:1000, Santa Cruz Biotechnology, Dallas, Texas, cat# SC-5538)

6. Magnetic Resonance Images (MRI)

To demonstrate anatomic and hemodynamic changes inside the AAA, 3-dimensional images of abdominal aorta were acquired at day 100 post-surgery with a ClinScan (Bruker/Siemens) 7 Tesla small animal MRI. Mice were anesthetized with isoflurance during the procedure. No vascular contrast was used during the procedure.

7. Statistical analysis

Distribution was tested by Shapiro-Wilk test of normality. Difference among groups was determined using Kruskal-Wallis nonparametric test. Post hoc Dunn's test was used for multiple comparisons between each two groups. Chi-square (and Fisher's exact) test was used for survival rate and AAA formation rate comparisons (PRISM 5, GraphPad Software, La Jolla, CA). Data are presented as mean ± standard deviation. P value less than 0.05 was considered statistically significant.

RESULTS

Aortic aneurysm characteristics, including significant rupture risk and presence of thrombus

In the BAPN Group, no aneurysm formation occurred at any time point, which provided a good negative base-line control for the other two groups. In the Elastase Group, primarily stage I aneurysms were observed on day 14 (125.9 ± 50.8%, $P < .01$ compared with BAPN Group). The average aortic diameter slightly decreased on day 21 and 28 (106.9 ± *26.5*% and 103.9 ± *30.4*% respectively), but remained positive to the end of study period (127.4 ± 41.6% on day 100). In the BAPN+Elastase Group, 1 mouse was excluded from the experiment for surgical complication). When compared the BAPN+Elastase Group with the Elastase Group, the two groups were similar in aortic diameter on day 14 (168.7 ± 53% vs 126 ± 50.8%, $P > .05$). In contrast, the AAAs in BAPN+Elastase Group demonstrated a persistent long-term growth trend (221.5 ± 36.6%, 285.8 ± 78.6%, 801 ± 160% on day 21, 28 and 100 respectively, $P < .001$ (Fig 2&3). The BAPN+Elastase Group also had a higher AAA formation rate (93% vs 65%, $P < .01$) and much more advanced stage AAAs (25/42 vs 1/40 at Stage II & III, $P < .001$) when compared with the Elastase Group. The differences looked more sizable after day 14 (Table I).

In the 100 day BAPN+Elastase mice, the aneurysms were not only large, many of them extended into the untreated suprarenal aorta and adjacent iliac, renal or gonadal arteries. They were also quite irregular in shape. The wall of those aneurysms was thick, but also had areas that were very thin or near rupture. More aneurysms were in stage III than in stage II. Of all the mice for this time point, 53.8 % (7/13) of them had thrombus (Fig 4). MRI images showed huge abdominal aneurysm of the infra-renal aorta with thrombi, demonstrating the dramatic anatomical and hemodynamic changes inside the AAA (Suppl 1). We did not find hind limb paralysis or other obvious symptoms on mice with thrombus. 46.2% of them (6/13) died of AAA rupture before the end of the experiment. Ruptures occurred on days 8, 8, 60, 74, 78 and 81 post-surgery, respectively (Fig 5). The ruptures seemed to occur at two intervals and had completely different features. Early ruptures (2/13) happened at the end of first week during the peak of acute inflammation. The shape of these rupture sites looked like a round “worm hole” with thick edge, located at the front wall of aorta (Fig 6A). In contrast, late ruptures (4/13 or 30.8%) happened between day 60 to 80 post-surgery. These ruptures were irregular in shape and were very thin walled, usually either on the back of aorta (Fig 6B) or on the affected smaller arteries, like gonadal artery. Out of these four late ruptured AAAs, three contained thrombus.

Histological characteristics of advanced stage AAA and chronic inflammation

In the BAPN+Elastsae Group, aortic wall thickening occurred earlier and was more prominent compared with the Elastase Group. In both groups, Verhoeff-Van Gieson staining demonstrated that the elastin in the media layer lost its wavy pattern with obvious fragmentation, especially of the internal elastic membrane. In the BAPN+Elastase Group, α-SMA staining showed that smooth muscle cells in the media also lost their circular and longitudinal layer arrangement, which should alternate with the layers of elastin fibers. There were large amounts of collagen deposited in the adventitia (Fig 7). In the 100 day

AAA samples with thrombus, the above changes were so extreme that the elastin and smooth muscle cells layers in the tunica media were almost lost completely (Fig 8). Neutrophil and macrophage infiltration in the aortic tissue peaked during the first week. The numbers of these acute inflammatory cells were negligible after two weeks. In contrast, the number of $CD3^+$ T cell in BAPN+Elastase Group increased remarkably after two weeks compared with Elastase Group (149 ± 37 vs 29 ± 16 on day 28 and 160 ± 76 vs 65 ± 10 on day 100, both $P < .01$), indicating persistent chronic inflammation in the later stages of aneurysm development (Fig 9).

Inflammatory cytokine profile

More than 50 cytokines were screened with cytokine and angiogenesis arrays (Table II). Most of inflammatory cytokines in the Elastase Group and the BAPN+Elastase Group peaked during the first 1–2 weeks after surgery and gradually declined toward the end of the experiment. When compared with the Elastase Group, certain cytokines in the BAPN +Elastase Group (pro-MMP9, IL-1β, IL-2, IL-6, IL-10, IL-13, CCL-3, CCL-5, CXCL-9 and TREM-1 etc.) were relatively higher on day 7 post-surgery, while others (IL-23, MCP-1 and TIMP-1) always maintained a higher level during the entire experiment (Suppl 2). Zymography, Western blot and ELISA were used to further quantify the selected cytokines according to the results of array screening. Increased pro-MMP2 activity was observed on day 21 and day 100 in BAPN+Elastase Group when compared with the Elastase Group ($P < .001$ and .05 respectively, Suppl 3). IL-1β, IL-6, TREM-1, CCL-5, MCP-1 and TIMP-1 levels were higher in BAPN+Elastase Group compared with the Elastase Group on day 7 post-surgery ($P < .05$, Suppl 4). There were no statistical differences for all the other cytokines at any time point between these two aneurysm groups (data not shown).

Age did not have effect on AAA diameter and incidence

Compared with 8-week old mice which are the standard age of mice used for AAA studies, the 18-month old mice seemed to have lower survival and AAA formation rate. Aortic dilation after aneurysm induction surgery was also milder. However, there were no statistical differences when comparing the younger mice in term of the aortic diameter or AAA incidence (Table III). Histological and cytokines profiles of the geriatric mice were also similar to their younger counterpart (data not shown).

DISCUSSION

An animal model of AAA should ideally possess all the features of human AAA. Of all the AAA experimental models to date, the elastase perfusion AAA model is the most widely used[11–12]. First described by Anidjar S et al in 1990 [1], and later characterized in great detail by Thompson RW et al [13], the model features an infrarenal dilated aortic segment with medial degeneration and adventitial inflammation similar to human AAA. However, like other AAA models, the elastase perfusion model does not exhibit many of the features of human aortic aneurysm. Most criticize the elastase perfusion model as an acute model, because the aneurysms primarily form during the second week after elastase perfusion, then gradually resolve over time, similar to a wound healing. This process is clearly different from human AAAs in that the patient's aneurysm occurs in a chronic fashion. In addition,

the impact of pressurized elastase perfusion on aorta is quite different from the injury that likely initiates human aneurysm formation.

While human aortic aneurysm is a disease of the elderly, the present study showed that mouse age had no effect on aneurysm development in elastase-induced AAA model. Similarly, Manninga MW et al also report that they did not note an effect of age of mice on AAA development when they investigated the variables to optimize Ang II model[14]. We speculated that human may be more susceptible to AAA compared with mice due to genetic differences.

In order to inhibit the animal's healing ability to mimic the geriatric condition in human, we treated the mice with 0.2% BAPN drinking water in our study. BAPN is an **irreversible** lysyl oxidase inhibitor that prevents the formation of lysine-derived aldehydes[15]. Lysyl oxidase(LOX) cross-links elastin and collagen fibers and plays a critical role in maintaining homeostasis of the elastic lamina[16–18].There was report that LOX expression progressively decreased after elastase perfusion in rat AAA model[19]. Similarly, a decrease of vascular LOX expression was observed in calcium chloride-induced AAA model[20]. In this model, vascular over-expression of LOX by local gene delivery normalizes aortic diameter and prevents AAA formation *in vivo*[20]. At present, there is no direct evidence showing that the LOX level in AAA patient's aorta is reduced, due to the difficulty of acquiring age-matched healthy aorta samples as control. But the recent data of human genetic study suggested that rare genetic variants in *LOX* predispose to thoracic aortic disease [21]. We also extended our study to 100 days after aneurysm induction to observe the long-term trend of AAA development.

In the traditional elastase-perfusion method, pressurized perfusion of the aorta is technically demanding and produces great variability in AAA size. This notorious technical variability makes the aortic dilation data incomparable among different surgeons or research groups. To eliminate this shortcoming, we replaced the pressurized perfusion with peri-aortic elastase application. This greatly simplifies the procedure and reduces technical variability. It also avoids the unnecessary ischemic-reperfusion injury during the traditional elastase perfusion of the aorta to the lower extremities.

Since the AAAs in our study had many new characteristics not often seen in other AAA models, aortic diameter measurement alone was not sufficient to describe all the AAA phenotype features. We therefore introduced a grading system to better characterize the different stages of aneurysm development. In our study, the AAAs induced by using elastase alone were relative mild (stage I). In contrast, the AAAs induced by the combination of BAPN and elastase application were very advanced (stage II & III). Giving enough time (e.g. 100 days in long-term mice), a significant amount of AAAs in this group eventually developed into the end-stage (stage III).

Compared with the traditional elastase perfusion model, our new AAA model has the following advantages: 1) Based mainly on the AAA phenotype development over time, it is a chronic, irreversible aneurysm with persistent growth into advanced stages; 2) the aneurysms in the model expand not only circumferencely, but also into adjacent intact

arteries; and 3) the aneurysms are irregular in shape and wall thickness with thrombus formation and spontaneous rupture. All of these are characteristics of human AAA, which are not seen in other AAA models. Additionally, the procedure is easy and practical with less technical variables and no ischemic-reperfusion injury. In addition, the size of AAA sample is quite large for a mouse model, which not only greatly improves the quality of bench analyses, but also is more efficient in saving research resources. Since this model can demonstrate all stages of aneurysm development, it is a very useful tool for aneurysm studies, especially for end stage AAAs with thrombus formation and spontaneous rupture.

In the present model, histological characteristics and inflammatory cytokine profiles of the Elastase Group and the BAPN+Elastase Group were very similar. But, elevated levels of MMP2 and $CD3^+$T cell accumulation during the late stages of AAA development in the BAPN+Elastase Group were the exceptions. MMP2 is known linked strongly to angiogenesis, tissue healing activity and aortic aneurysm rupture. $CD3^+$T cells accumulation is also associated with chronic inflammation in our model and may be the target of future studies. Our results also suggest that the initial acute inflammation caused by the aneurysm induction surgery lasts about 2 weeks and this period should be avoided. If the purpose of the study is for early stage AAA formation, 2–4 weeks after the induction surgery probably would be better time frame. For those studies focused on the end stage tissue re-modeling, observations may need to be extended beyond 60 days in order to have significant thrombus formation and spontaneous rupture.

There are other AAA models used in aneurysm research. The blotchy mice develop spontaneous aortic aneurysms/dissection due to the deficiency in elastin and collagen cross-linking [1]. However, the generalized metabolic alterations caused by this gene defect restrict its application. AAAs from the calcium chloride induced model [(3)] are small in general (only obtains a great than 50% dilation), hardly being considered as true aneurysms. The angiotensin II model also been used for aneurysm studies in recent years[4–6]. However, the main mechanism of AAA formation induced by Angiotensin II is secondary to aortic dissection, which is quite different from human aortic aneurysm formation. Combination of BAPN with Ang II significantly improved the incidence of aneurysm formation. But, the earlier BAPN models[22–23] were designed mainly to mimic the acute aortic dissection in human. All the dissections/or ruptures in those models happened in the acute phase of aneurysm induction (e.g. within a week). Aortic aneurysms in the Angiotensin II model also occur in the suprarenal aortic segment, whereas most of the human AAAs occurs in the infrarenal segment. Additionally, the Angiotensin II model was originally designed to use apolipoprotein E deficient mice for the study of atherosclerosis. More studies are needed to prove the feasibility of using wild type mice in Angiotensin II model for AAA experiments.

We recently used a BAPN+Elastase rat perfusion model for AAA rupture study[22]. However, the AAA ruptures in that study occurred just 6 to 8 days following perfusion, which likely were the result of acute inflammation. Since the goal of this experiment is to establish a “chronic” AAA model, the BAPN amount used was considerably lower than our rat AAA rupture model or the acute aortic dissection model[22–23]. Adaptation of BAPN+Elastase model in standard C57BL/6 mice will enable future studies to be performed in more genetically modified strains to explore the sophisticated mechanisms of aneurysm formation.

More importantly, it is truly a chronic AAA model, which possesses more characteristics of human AAA than any other AAA model to date.

Human aortic ruptures mostly happen as an ending result of aneurysm development. In our model, the spontaneously ruptures in the later stages of AAA development were quite similar to human AAA rupture. Furthermore, the authors believe that the more logical explanation of aneurysm formation in human should be the co-existence of both the initial injury and impaired repair ability (e.g. as demonstrated in this experiment).

The present experiment also demonstrated that different of BAPN dosages may lead to different degree of repair deficiency, hence to different pathological phenotype. The amount of BAPN in our experiment was lower compared with the other BAPN models in the past[19,22–23] Most of the late ruptures happened in the ending stage of aneurysm development, with only a few early ruptures. For a chronic AAA model, it is a challenge to find an adequate BAPN dosage to balance the early dissection (or rupture) that we don't want and later ruptures that we really need. We'll fine-tune the BAPN dosage in the future to further improve this useful chronic model. Of course, the detail mechanisms of late-staged AAA development also need to be explored with pharmacologic therapies aimed at reducing the chronic process in human AAAs.

CONCLUSION

A chronic, advanced stage AAA mouse model was established using a combination of BAPN administration and peri-aortic elastase application. The basic histological and cytokine profile was characterized. This new AAA mouse model has many advantages over multiple models used at present. It is especially a useful and powerful tool for studying tissue re-modeling, thrombus formation and aneurysm rupture that occurs during the end stage of AAA development.

Supplementary Material

Refer to Web version on PubMed Central for supplementary material.

Acknowledgments

Source of funding: This work was supported by NIH RO1 HL081629 (G.R.U).

References

1. Andrews EJ, White WJ, Bullock LP. Spontaneous aortic aneurysms in blotchy mice. Am J Pathol. 1975; 78(2):199–208. [PubMed: 1115218]
2. Anidjar S, Salzmann JL, Gentric D, Lagneau P, Camilleri JP, Michel JB. Elastase-induced experimental aneurysm in rat. Circulation. 1990; 82:973–981. [PubMed: 2144219]
3. Chiou AC, Chiu B, Pearce WH. Murine aortic aneurysm produced by periarterial application of calcium chloride. J Surg Res. 2001; 99:371–376. [PubMed: 11469913]
4. Daugherty A, Manning MW, Cassis LA. Angiotensin II promotes atherosclerotic lesions and aneurysms in apolipoprotein E-deficient mice. J Clin Invest. 2000; 105:1605–12. [PubMed: 10841519]

5. Daugherty A, Cassis LA. Mouse models of abdominal aortic aneurysms. ATVB Biol. 2004; 24:429–434.
6. Kanematsu Y, Kanematsu M, Kurihara C, Tsou TL, Nuki Y, Liang EI, et al. Pharmacologically induced thoracic and abdominal aortic aneurysms in mice. Hypertension. 2010; 55:1267–1274. [PubMed: 20212272]
7. Lau CL, Zhao Y, Kron IL, Stoler MH, Laubach VE, Ailawadi G, et al. The role of adenosine A2A receptor signaling in bronchiolitis obliterans. Ann Thorac Surg. 2009; 88(4):1071–8. [PubMed: 19766783]
8. Zhao Y, LaPar DJ, Steidle J, Emaminia A, Kron IL, Ailawadi G, et al. Adenosine signaling via the adenosine 2B receptor is involved in bronchiolitis obliterans development. J Heart Lung Transplant. 2010; 29(12):1405–14. [PubMed: 20920842]
9. Zhao Y, Xiao A, diPierro CG, Carpenter JE, Abdel-Fattah R, Redpath GT, et al. An extensive invasive intracranial human glioblastoma xenograft model: role of high level matrix metalloproteinase 9. Am J Pathol. 2010; 176(6):3032–49. [PubMed: 20413683]
10. DiMusto PD, Lu G, Ghosh A, Roelofs KJ, Su G, Zhao Y, et al. Increased PAI-1 in females compared with males is protective for abdominal aortic aneurysm formation in a rodent model. Am J Physiol Heart Circ Physiol. 2012; 302(7):1378–86.
11. Lu G, Su G, Zhao Y, Johnston WF, Sherman NE, Rissman EF, et al. Dietary phytoestrogens inhibit experimental aneurysm formation in male mice. J Surg Res. 2014; 188(1):326–338. [PubMed: 24388399]
12. Johnston WF, Salmon MD, Pope NH, Meher A, Su G, Stone ML, et al. Inhibition of interleukin-1b decreases aneurysm formation and progression in a novel model of thoracic aortic aneurysms. Circulation. 2014; 130:S51–S59. [PubMed: 25200056]
13. Thompson RW, Curci JA, Ennis TL, Mao D, Pagano MB, Pham CTN, et al. Pathophysiology of abdominal aortic aneurysms: Insights from the elastase-induced model in mice with different genetic backgrounds. Ann NY Acad Sci. 2006; 1085:59–73. [PubMed: 17182923]
14. Manning MW, Cassi LA, Huang J, Szilvassy SJ, Daugherty A. Abdominal aortic aneurysms: fresh insights from a novel animal model of the disease. Vasc Med. 2002; 7(1):45–54. [PubMed: 12083734]
15. Siegel RC, Martin GR. Collagen crosslinking: enzymatic formation of lysine derived aldehydes and the production of crosslinked components. J Biol Chem. 1970; 245:1653–1658. [PubMed: 5438356]
16. Moursi MM, Beebe HG, Messina LM, Welling TH, Stanley JC. Inhibition of aortic aneurysm development in blotchy mice by beta adrenergic blockade independent of altered lysyl oxidase activity. J Vasc Surg. 1995; 21(5):792–9. [PubMed: 7769737]
17. Mäki JM, Räsänen J, Tikkanen H, Sormunen R, Mäkikallio K, Kivirikko KI, et al. Inactivation of the Lysyl Oxidase Gene *Lox* Leads to Aortic Aneurysms, Cardiovascular Dysfunction, and Perinatal Death in Mice. Circulation. 2002; 106:2503–2509. [PubMed: 12417550]
18. Hornstra IK, Birge S, Starcher B, Bailey AJ, Mecham RP, Shapiro SD. Lysyl oxidase is required for vascular and diaphragmatic development in mice. J Biol Chem. 2003; 278(16):14387–93. [PubMed: 12473682]
19. Huffman MD, Curci JA, Moore G, Kerns DB, Starcher BC, Thompson RW. Functional importance of connective tissue repair during the development of experimental abdominal aortic aneurysms. Surgery. 2000; 128(3):429–38. [PubMed: 10965315]
20. Yoshimura K, Aoki H, Ikeda Y, Furutani A, Hamano K, Matsuzaki M. Regression of abdominal aortic aneurysm by inhibition of c-Jun N-terminal kinase in mice. Ann N Y Acad Sci. 2006; 1085:74–81. [PubMed: 17182924]
21. Guo DC, Regalado ES, Gong L, Duan X, Santos-Cortez RL, Arnaud P, et al. LOX Mutations Predispose to Thoracic Aortic Aneurysms and Dissections. Circ Res. 2016; 118(6):928–34. [PubMed: 26838787]
22. English SJ, Piert MR, Diaz JA, Gordon D, Ghosh A, D'alecy LG, et al. Increased 18F-FDG uptake is predictive of rupture in a novel rat abdominal aortic aneurysm rupture model. Ann Surg. 2015; 261(2):395–404. [PubMed: 24651130]

23. Kurihara T, Shimizu-Hirota R, Shimoda M, Adachi T, Shimizu H, Weiss SJ, et al. Neutrophil-Derived Matrix Metalloproteinase 9 Triggers Acute Aortic Dissection. Circulation. 2012; 126:3070–3080. [PubMed: 23136157]

Clinical Relevance

A chronic AAA animal model is described, which possesses more characteristics of human AAA compared with other AAA models. Since this model demonstrates all stages of aneurysm formation, it is a very useful tool for investigational aneurysm studies, especially for end-stage AAA with thrombus formation and spontaneous rupture. It also can be performed in genetically modified strains to explore the sophisticated mechanisms of aneurysm formation.

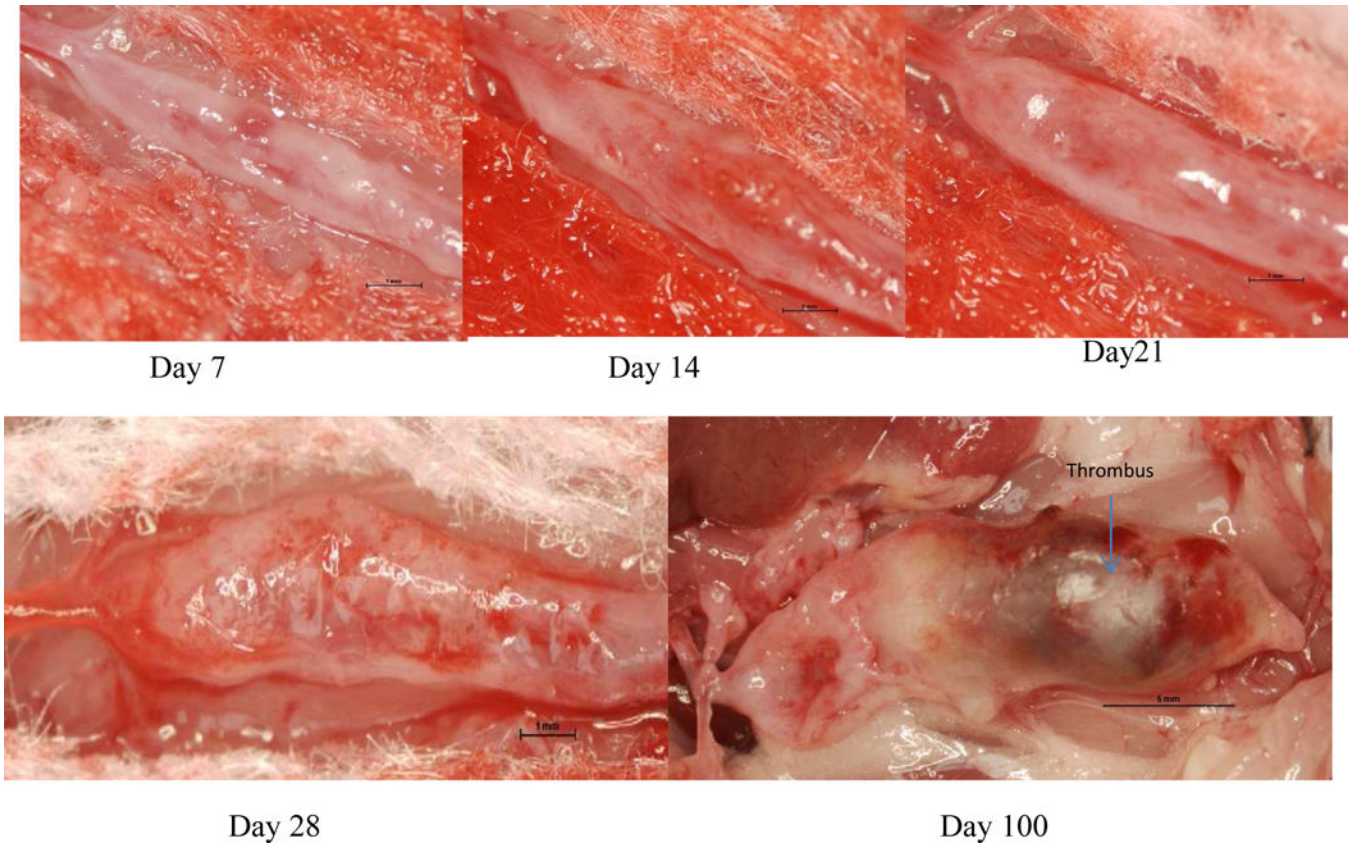

Fig 1.

Representative AAA samples at different stages of aneurysm development in BAPN +Elastase induced model. Day 7, 14 & 21— stage I; Day 28 — stage II; Day 100 — stage III.

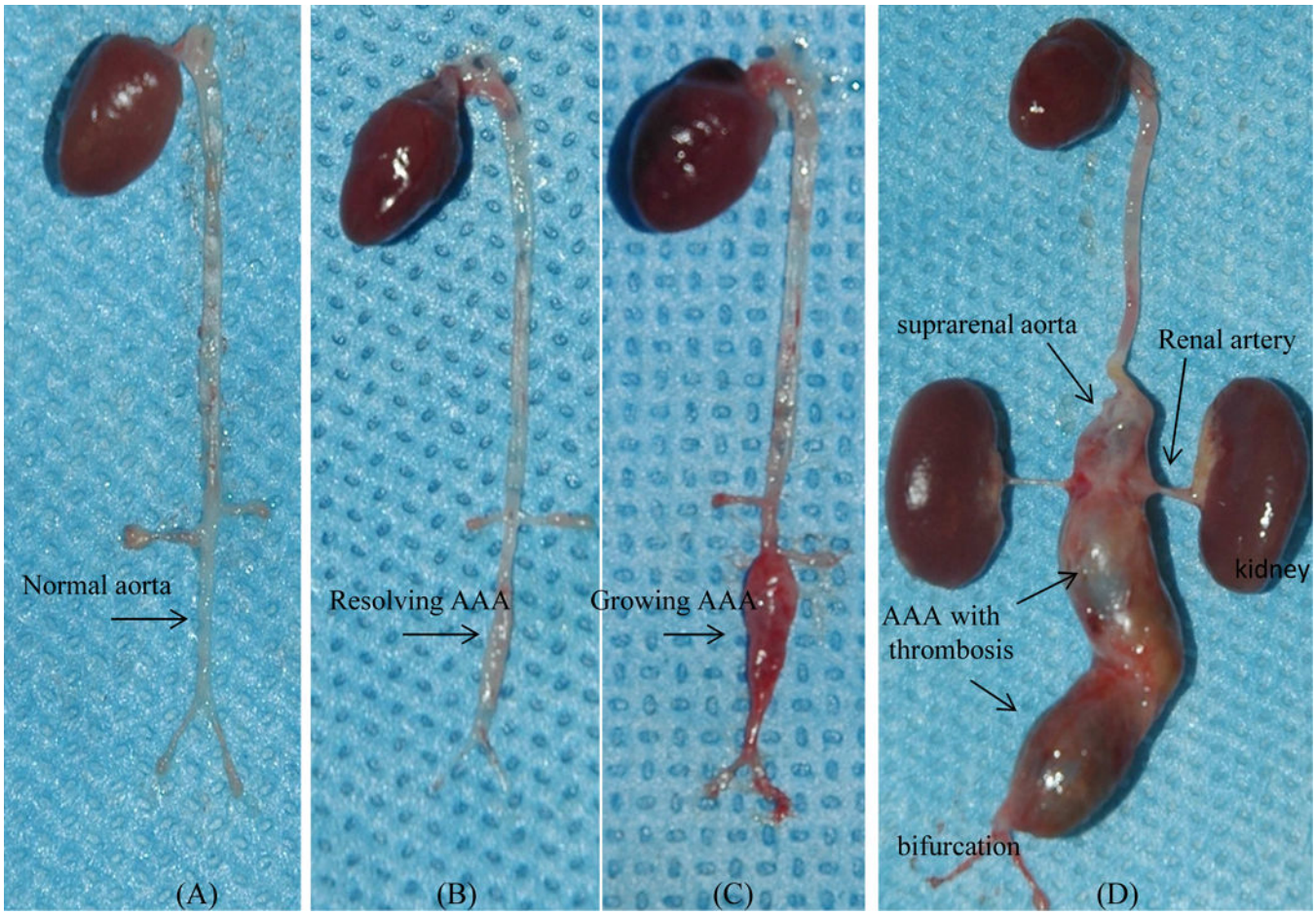

Fig 2.

Comparison of representative samples on post-surgery day 28: BAPN Group (A) showed normal infrarenal aorta; In Elastase Group (B), aortic aneurysm almost resolved by itself, but scaring tissue on infrerenal aorta was still visible; In contract, aortic aneurysm in BAPN +Elastase Group (C) kept growing on the same period. On 100 day post-surgery, huge aortic aneurysms in the BAPN+Elastase Group (D) expanded to suprarenal aorta.

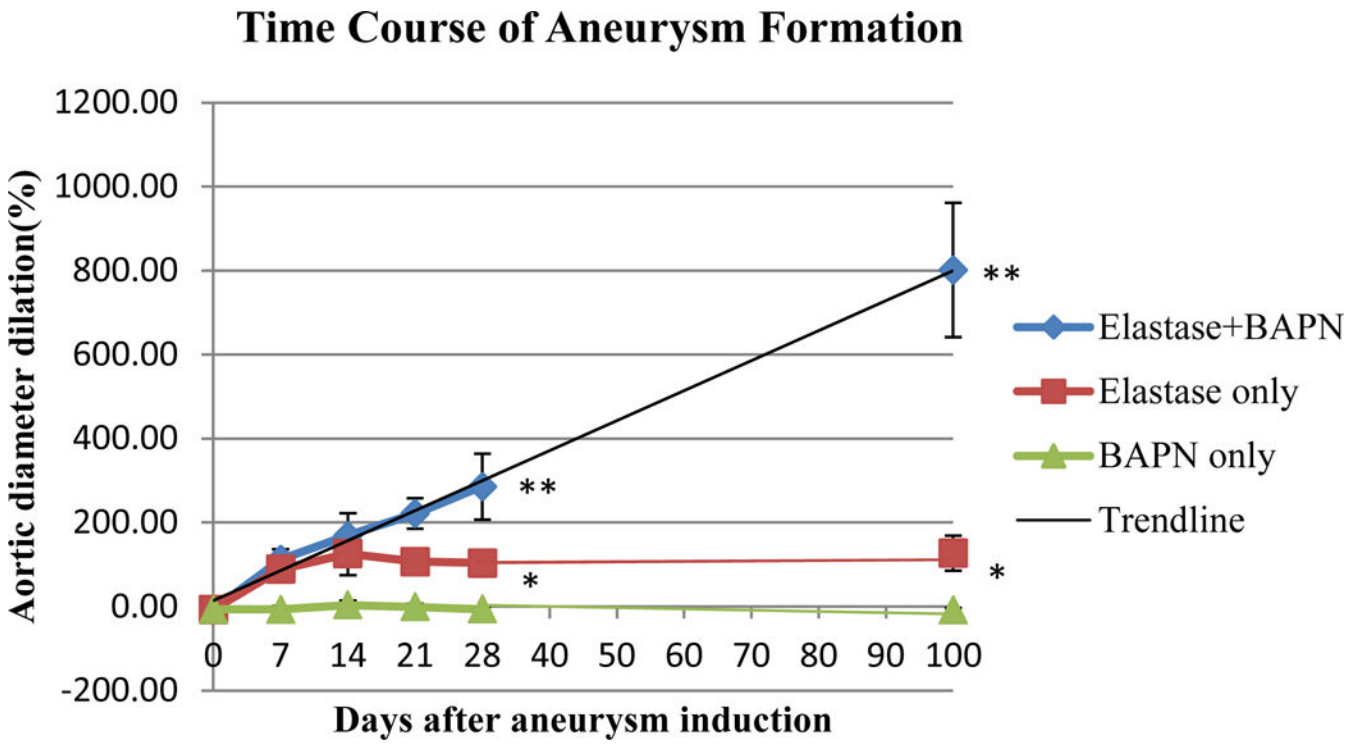

Fig 3.

Comparison of aortic aneurysm diameter of three groups (n=8 mice for each point). Aortic aneurysm in BAPN+Elastase Group showed a persistent long-term growing trend. *BAPN Group compared with Elastase Group: P < .001, **BAPN+Elastase Group compared with Elastase Group: P < .001

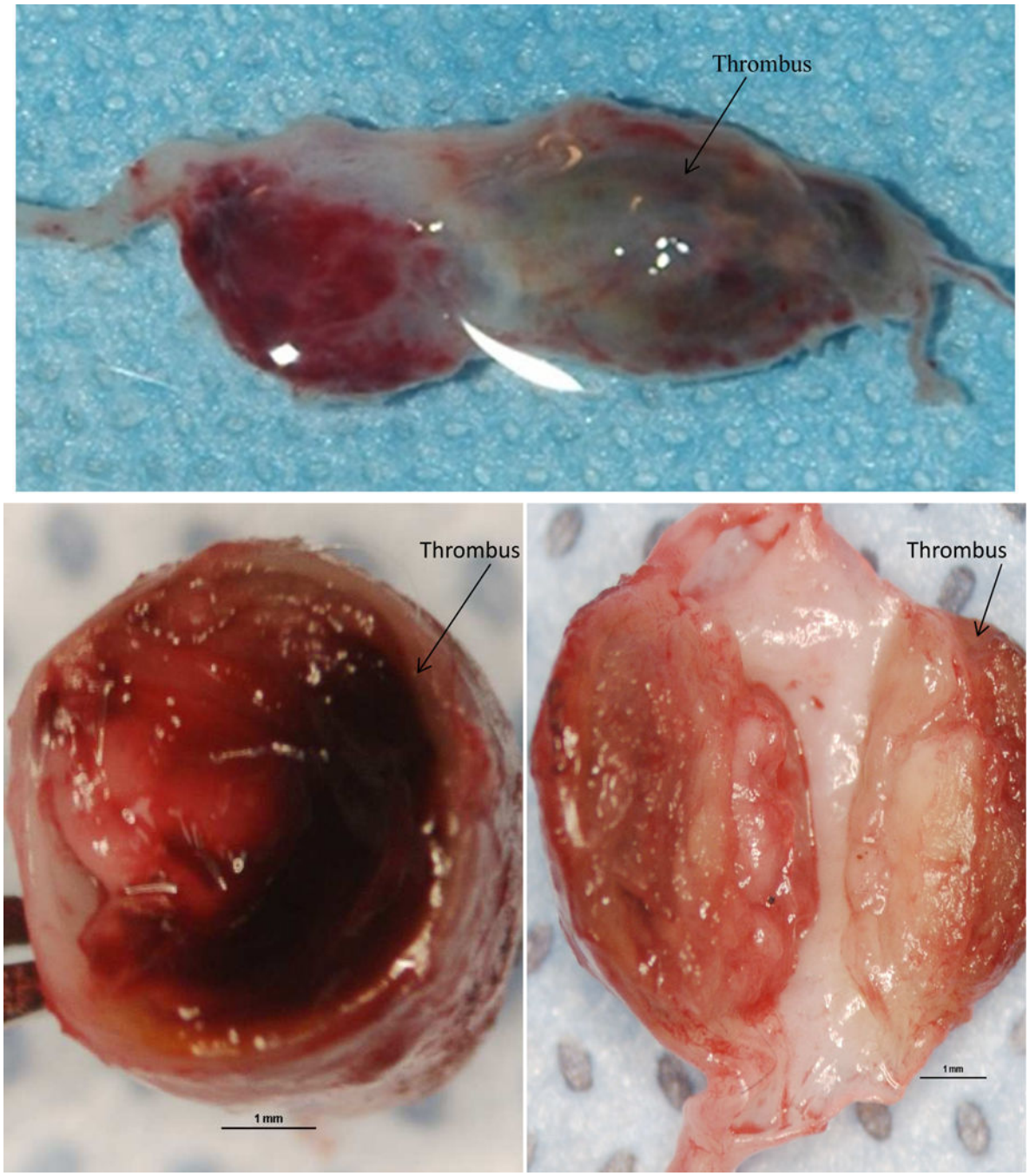

Fig 4.

Aortic aneurysm sample (stage III) from 100 day BAPN+Elastase Group. Above: Aortic aneurysm with thrombus inside. Below: Cross section of aneurysm showed very thick wall with thrombus (arrow).

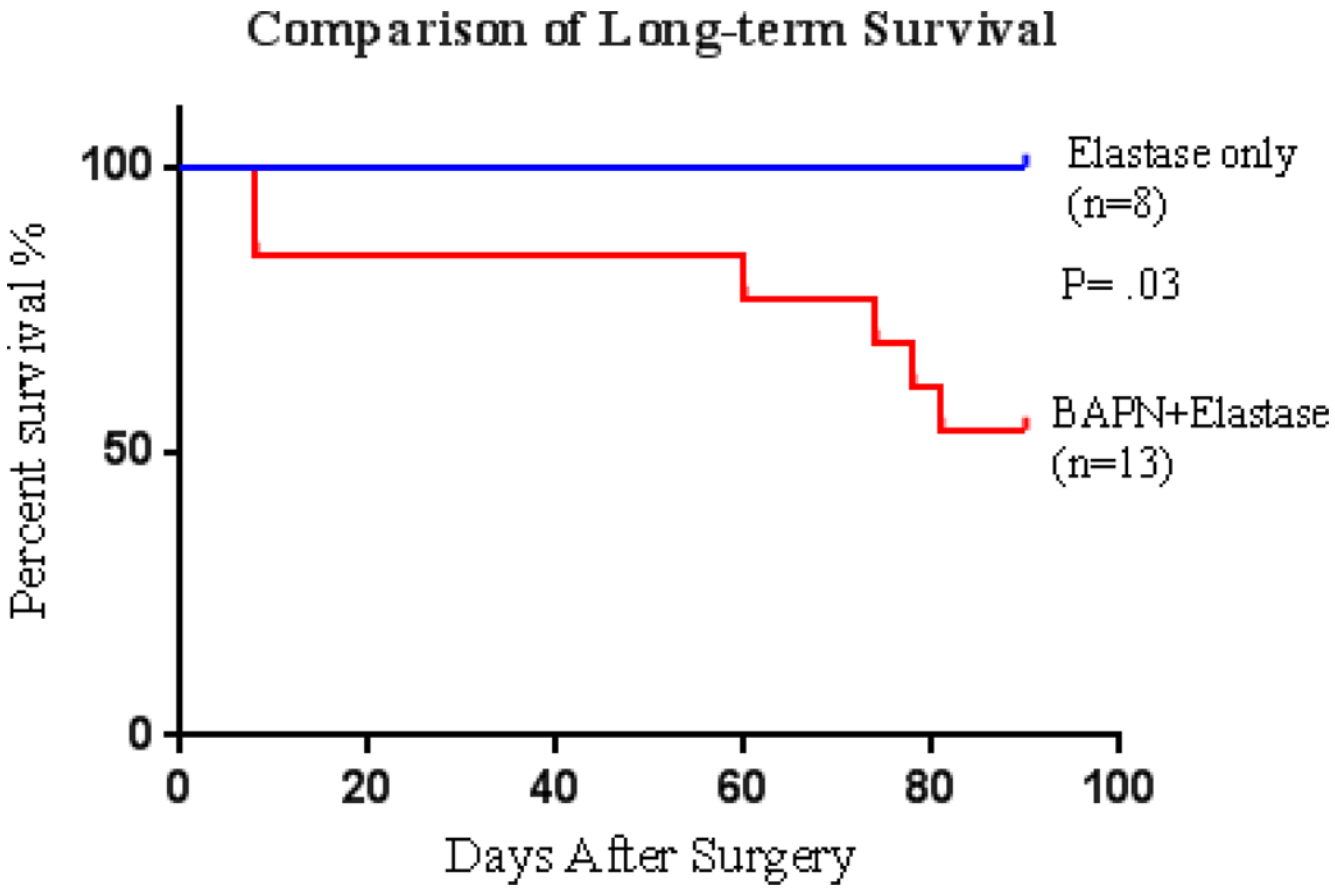

Fig 5.

Aneurysm ruptures in BAPN+Elastase Group occurred at the end of first week and 60 days after surgery.

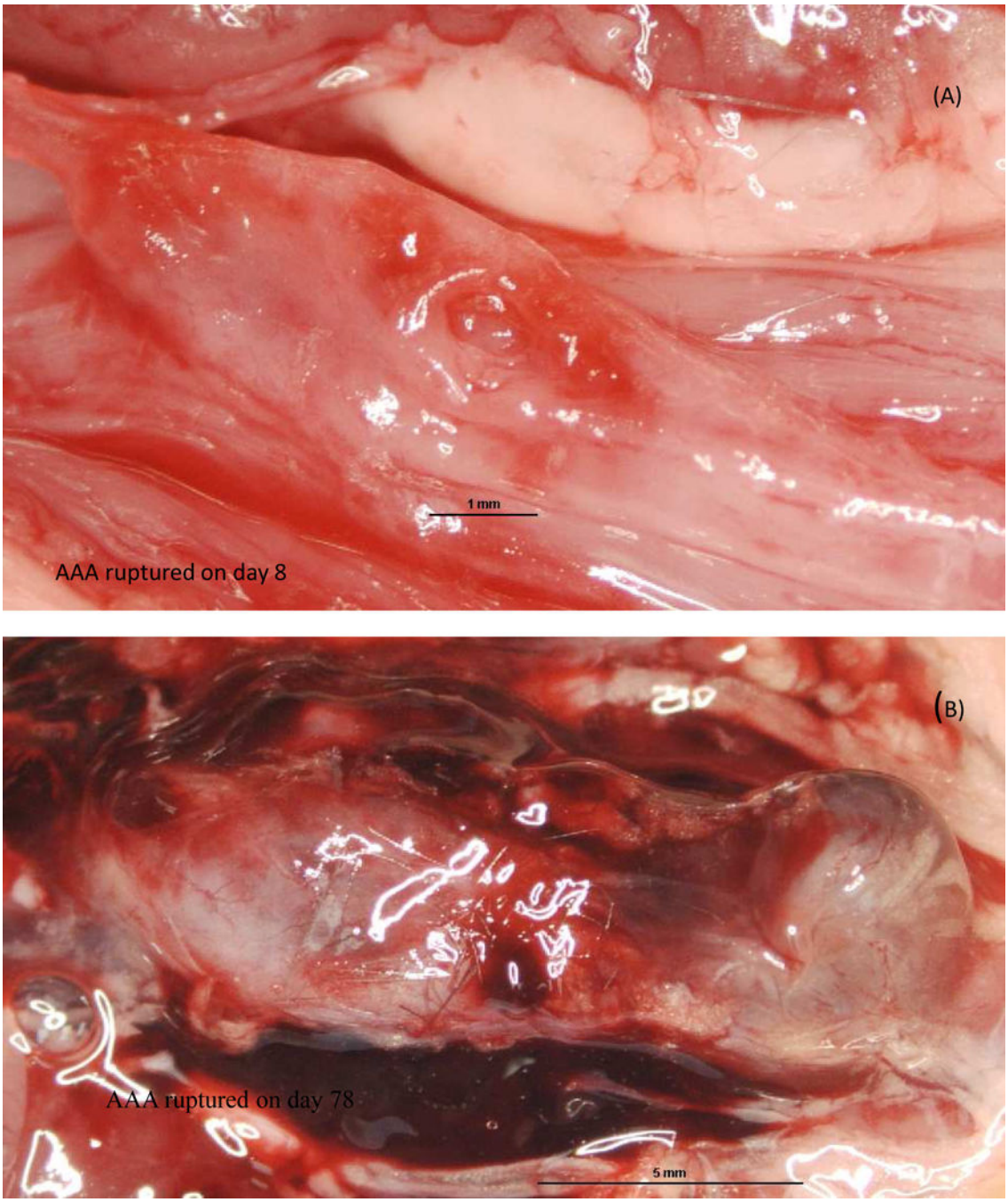

Fig 6.

Ruptured aortic aneurysm in BAPN+Elastase Group. (A): early stage rupture - fusiform aneurysm with a rupture site on the front wall as marked by arrow. (B): late stage ruptur - Irregular shape aneurysm with obvious fibrillization and thrombus formation. Rupture site on the back of aneurysm (not shown). Hemorrhage was contained in the retroperitoneum.

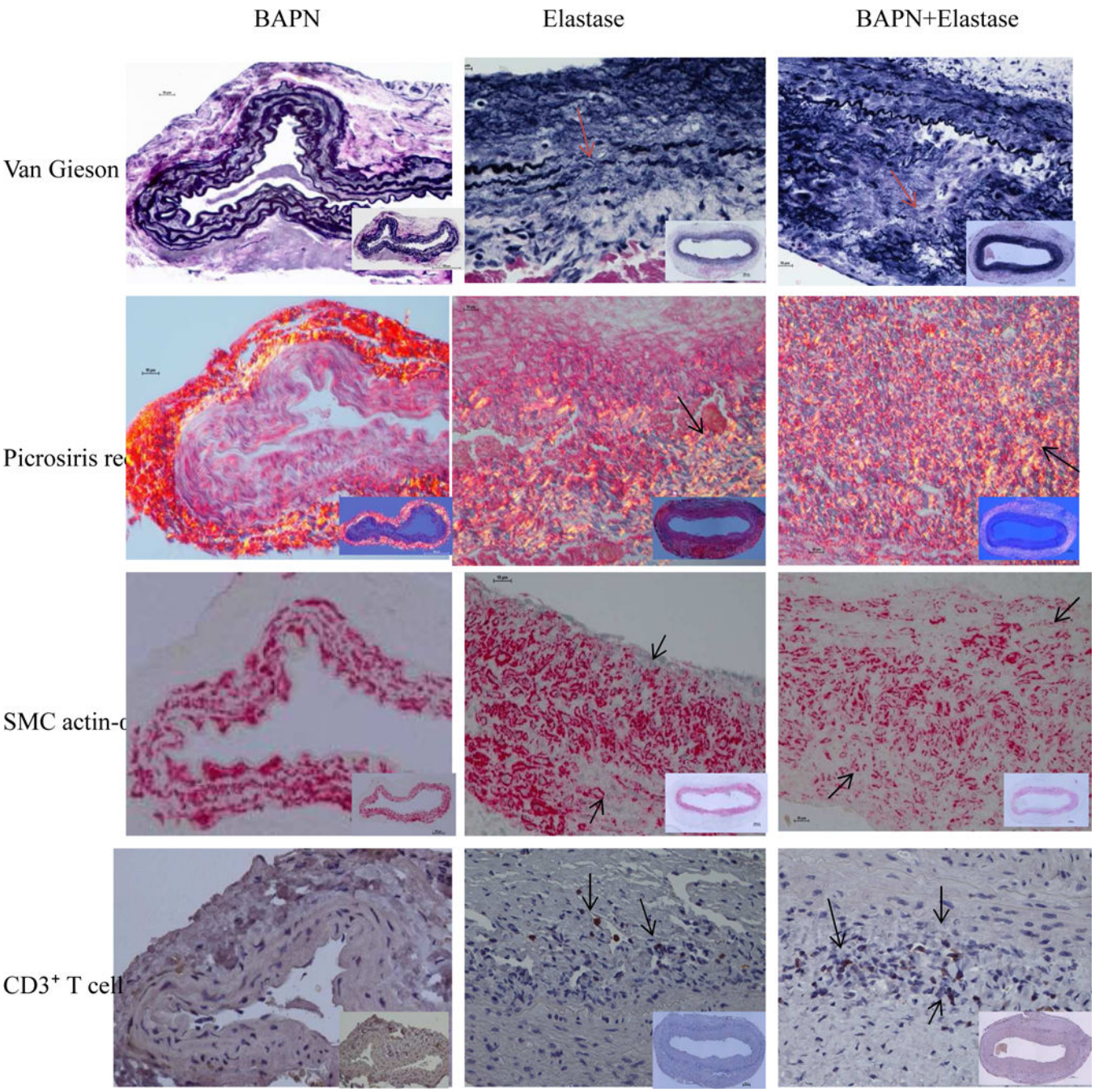

Fig 7.

Comparison the composition of elastin (Van Gieson), collagen (Picrosiris red), smooth muscle cell (SMC actin-α) and $CD3^+$ T cells in different groups. Representative samples on post-operative day 28. BAPN+Elastase Group samples had obvious elastin fragmentation and large amounts of collegan deposition; Smooth muscle cells also lost their normal layered arrangement. The structural changes in Elastase Group sample was similar, but less severe than BAPN+Elastase Group. The $CD3^+$ T cells in the BAPN+Elastase Group was increased significantly compared with the other groups. Magnification: 40X (insert 10X).

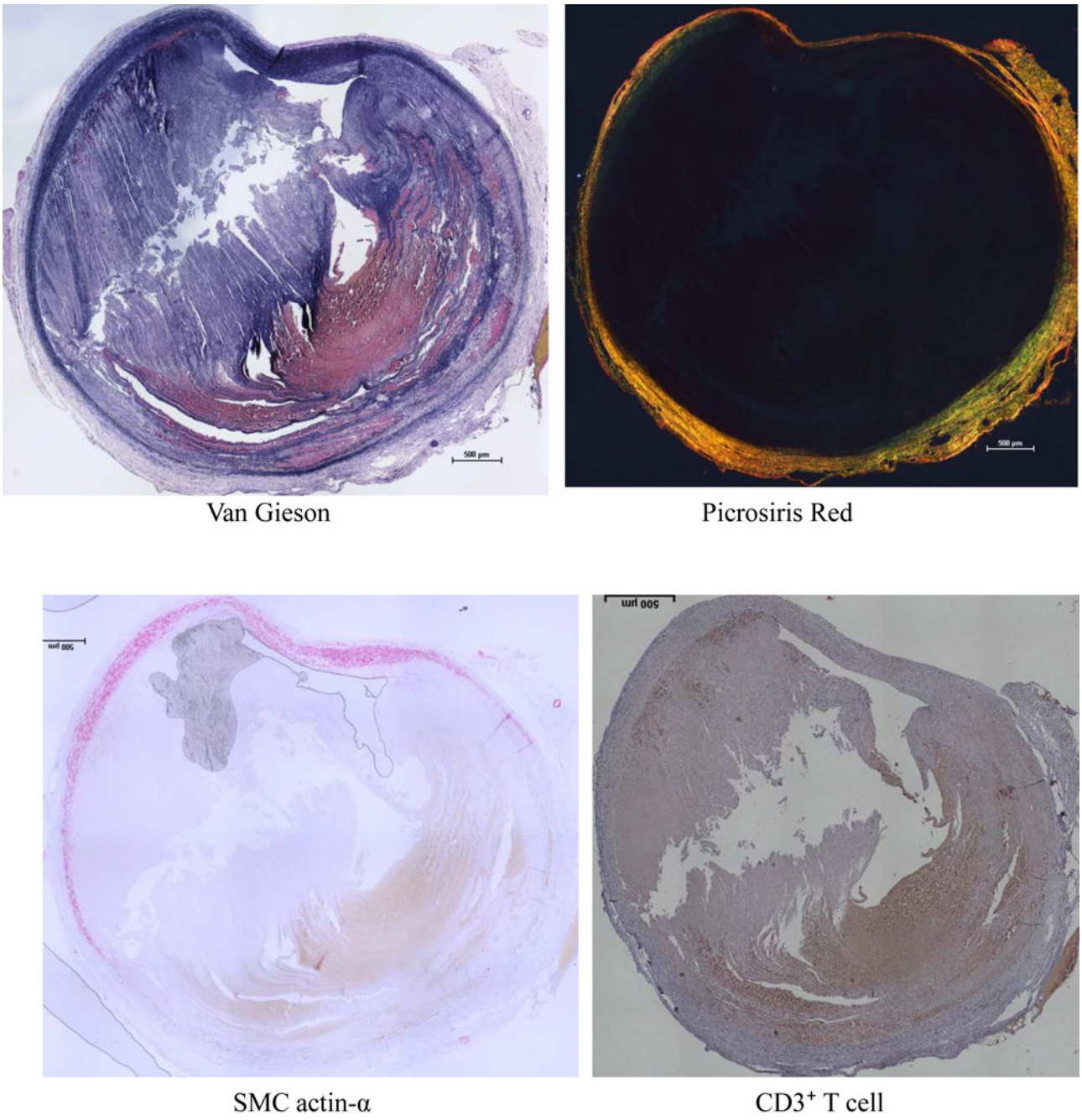

Fig 8.

Thrombus formation in 100 day AAA sample from BAPN+Elastase Group. Huge thrombus occupied most part of the vessel. In the extremely dilated aortic wall, most of the elastin lamellæ and smooth muscle cells in the tunica media was lost and replaced by collagen deposition and $CD3^+$ T cell infiltration.

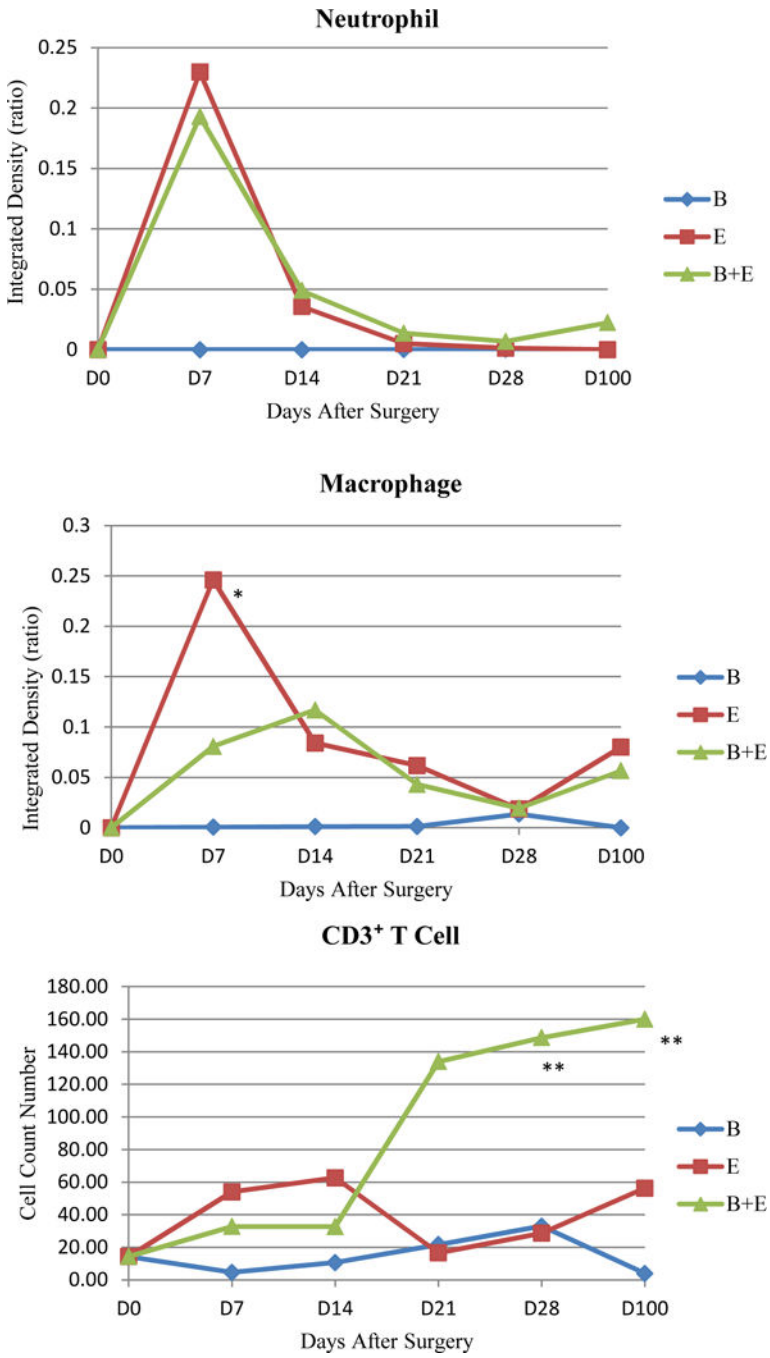

Fig 9.

Comparison of inflammatory cells in three groups at multiple time points. The number of lymphocytes in BAPN+Elastase Group increased peaked on day 28 post-surgery. BAPN +Elastase Group compared with Elastase Group * P < .05, ** P < .01.

Table I

Comparison of AAA formation rate & stage in different groups. BAPN+Elastase Group had higher AAA rate and much more advanced-stage aneurysms than Elastase Group.

	Aneurysm	Day 7	Day 14	Day 21	Day 28	Day 100
BAPN only	AAA rate	0%	0%	0%	0%	0%
	Stage −	8	8	8	8	8
Elastase only	AAA rate	25%	87.5%	62.5%	75%	75%
	Stage −	6	1	3	2	2
	Stage +	2	6	5	6	6
	Stage ++		1			
BAPN+Elastase	AAA rate	75%	85.7%	100%	100%	100%
	Stage −	2	1			
	Stage +	6	4	3	1	
	Stage ++		2	5	7	3
	Stage +++					8

Grading Standard:

−negative: Symmetric dilation <100%, thin wall, no thrombosis/rupture.

†stage I: Symmetric dilation between 100–200%, thick wall, no thrombosis/rupture.

††stage II: Asymmetric dilation >200%, thick/uneven wall, no thrombosis/rupture.

†††stage III: stage II plus thrombosis/rupture.

Table II

Summary of cytokine activities in different periods of experiment.

Cytokines peaked at the first week: pro-MMP9 [a], act-MMP9, act-MMP2, INF-r [a], TNF-a [a], IL-1β [a], IL-1Ra, IL-2 [a], IL-5, IL-6 [a], IL-10 [a], IL-13[a], IL-16, IL-17, IL-23 [b], IL-27, CCL-2 [b], CCL-3 [a], CCL-5[a], CCL-11, CCL-17, CXCL-1[a], CXCL-2, CXCL-9[a], CXCL-10, CXCL-11, CXCL-13, G-CSF, GM-CSF, TIMP-1 [b], TREM-1[a]
Cytokines peaked at the second week: IL-1a, IL-3, IL-4, IL-7 CCL-1, CCL-4, CCL-12, CXCL-12 M-CSF, CD45, C5a, PAI-1, AKT, p-AKT, MMP8, t-PA, u-PA, JNK, p-JNK
Cytokines peaked after 2 weeks: Pro-MMP2[a], IL-12p70

[a]Cytokine level in BAPN+Elastase Group was relatively higher than Elastase Group on day 7 post-surgery.

[b]Cytokine level in BAPN+Elastase Group was relatively higher than Elastase Group at all the time points during the experiment.

MMP: matrix metalloproteinase. INF-r: *interferon-r*, TNF-a: tumor necrosis factor-a. IL: interleukin. CCL: chemokine (C-C motif) ligand. CXCL: chemokine(C-X-C motif) ligand. G-CSF: granulocyte-colony stimulating factor. TIMP-1: tissue inhibitor of metalloproteinases-1. TREM-1: triggering receptor expressed on myeloid cells 1. PAI-1: plasminogen activator inhibitor-1. AKT: protein kinase B. t-PA: Tissue plasminogen activator. U-PA: *cytokine*-regulated urokinase-type-plasminogen-activator. JNK: c-Jun N-terminal kinase.

Table III

Comparison of elastase-induced AAA in young mice with different geriatric mice groups at day 14 post-surgery. The survival rate, incidence of AAA rate and aortic diameter seemed lower as the mice grew older, but there were no statistical differences among groups (P > .05).

Age Group	2 months	6 months	12 months	18 months
Total of mice	6	6	6	8
Survival (%)	100 (6/6)	100 (6/6)	83.3 (5/6)	62.5 (5/8)
AAA incidence (%)	83.3 (5/6)	66.7 (4/6)	60 (3/5)	20 (1/5)
Aortic Diameter (%)	121.5±41.5	127.5±53.5	120.2±40.6	80.2±38.2
Statistics	ns	ns	ns	ns